Launching of Davydov solitons in protein α-helix spines

Danko D. Georgiev[a,*], James F. Glazebrook[b]

[a]*Institute for Advanced Study, 30 Vasilaki Papadopulu Str., Varna 9010, Bulgaria*
[b]*Department of Mathematics and Computer Science, Eastern Illinois University, Charleston, IL 61920, USA*

Abstract

The biological order provided by α-helical secondary protein structures is an important resource exploitable by living organisms for increasing the efficiency of energy transport. In particular, self-trapping of amide I energy quanta by the induced phonon deformation of the hydrogen-bonded lattice of peptide groups is capable of generating either pinned or moving solitary waves following the Davydov quasiparticle/soliton model. The effect of applied in-phase Gaussian pulses of amide I energy, however, was found to be strongly dependent on the site of application. Moving solitons were only launched when the amide I energy was applied at one of the α-helix ends, whereas pinned solitons were produced in the α-helix interior. In this paper, we describe a general mechanism that launches moving solitons in the interior of the α-helix through phase-modulated Gaussian pulses of amide I energy. We also compare the predicted soliton velocity based on effective soliton mass and the observed soliton velocity in computer simulations for different parameter values of the isotropy of the exciton–phonon interaction. The presented results demonstrate the capacity for explicit control of the soliton velocity in protein α-helices, and further support the plausibility of gradual optimization of quantum dynamics for achieving specialized protein functions through natural selection.

Keywords: Davydov soliton, energy transport, phase modulation, protein function, quantum dynamics

1. Introduction

Proteins play a diverse number of roles in living organisms. In the impressive portfolio of protein assignments, the most important are the following: catalytic, structural, contractile, regulatory, protective, and transportation. The biological value of proteins is paramount for organisms when passing the former to their offspring, in the form of hereditary DNA information, to the extent that exact amino acid sequences of the proteins have already ensured the success of the parent organism. Each of the listed protein functions is performed at the expense of free biochemical energy and is supported by highly evolved specialized protein structural motifs. While the dynamics of all biomolecules is fundamentally governed by quantum mechanical laws, the highly efficient utilization of individual energy quanta by proteins suggests that characteristic quantum effects may be indispensable for a deeper understanding of the mechanisms of life [1].

Protein α-helices constitute a common motif in the secondary structure of proteins [2–4]. Each α-helix is a right-handed spiral with 3.6 amino acid residues per turn [5, 6]. The helical structure is stabilized by hydrogen bonding between the N–H group from an amino acid and the C=O group from another amino acid located four residues earlier in the primary amino acid sequence of the protein. This bonding produces three parallel chains of hydrogen-bonded peptide groups referred to as α-helix spines [6]. The interaction between C=O bond stretching (amide I excitons) and the deformation of the lattice of –C=O$\cdots$H–N– hydrogen bonds (phonons) provides a quantum model for the transport of energy in terms of Davydov solitons [7–16].

For a single α-helix spine of hydrogen-bonded peptide groups, the generalized Davydov model describes the quantum dynamics of amide I excitons, lattice phonons, and the nonlinear exciton–phonon interaction

---

[17–36]. The system of gauge transformed quantum equations of motion is [1]

$$\imath\hbar\frac{d}{dt}a_n = -J_{n+1}a_{n+1} - J_n a_{n-1} + \chi\left[b_{n+1} + (\xi-1)b_n - \xi b_{n-1}\right]a_n \tag{1}$$

$$M_n\frac{d^2}{dt^2}b_n = w\left(b_{n-1} - 2b_n + b_{n+1}\right) - Q\chi\left(|a_{n-1}|^2 + (\xi-1)|a_n|^2 - \xi|a_{n+1}|^2\right) \tag{2}$$

where Q is the number of excited amide I quanta, a_n is the amide I quantum probability amplitude at the nth peptide group, $\hbar$ is the reduced Planck constant, J_n is the dipole–dipole coupling energy between the nth and $(n-1)$th amide I oscillator along the α-helix spine, b_n is the phonon displacement of the nth peptide group from its equilibrium position, M_n is the mass of the nth peptide group, w is the spring constant of the hydrogen bonds in the lattice [8, 9, 33], $\chi = \bar{\chi}\frac{2}{1+\xi}$ is a nonlinear coupling parameter between the amide I exciton and the phonon displacements of peptide groups in the lattice of hydrogen bonds, $\bar{\chi} = \frac{\chi_r + \chi_l}{2}$, χ_r and χ_l couple the amide I oscillator (C=O group) with the hydrogen bonds ($\cdots$) respectively to the right or to the left in the chemical structure of the α-helix spine

$$\cdots H - N - C = O\underbrace{\cdots H - N - C =}_{\chi_l}O\underbrace{\cdots H}_{\chi_r} - N - C = O \cdots$$
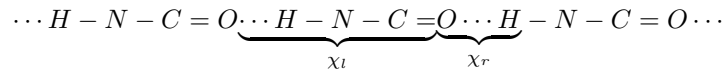
and $\xi = \frac{\chi_l}{\chi_r}$ is the anisotropy parameter of the exciton–phonon interaction (in proteins $\chi_r > 0$ and $0 \leq \chi_l \leq \chi_r$ thereby constraining ξ in the interval $[0,1]$) [6, 35, 37]. For a complete derivation of the system of quantum equations of motion, we refer the interested reader to Ref. [1].

Most biochemical processes in living organisms are driven by free energy as provided by the cleavage of pyrophosphate bonds in adenosine triphosphate (ATP). ATP hydrolysis to adenosine diphosphate (ADP) and orthophosphate (P_i) releases 0.41 eV of free energy. Thus, for every ATP molecule utilized, proteins are able to excite $Q = 2$ amide I quanta, each of which carries 0.205 eV.

In order to study the mechanisms for launching of Davydov solitons, which represent traveling solitary waves of amide I energy dressed by an accompanying phonon deformation in the protein α-helix, we have integrated numerically the system of Davydov equations (1) and (2) using uniform values J and M for all peptide groups n. For enhancement of the accuracy and speed of computational simulations, we performed the numerical integration with LSODA, Livermore Solver for Ordinary Differential equations with Automatic selection between nonstiff (Adams) and stiff (Backward Differentiation Formula, BDF) methods [37–41].

The main problems that we address in this present computational study are: Is it possible to generate Davydov solitons without an initial phonon dressing? Is there a physical mechanism that would allow proteins to launch Davydov solitons in the interior of protein α-helices? Is the higher flux of amide I energy quanta capable of supporting Davydov solitons in protein conformations with weak nonlinear exciton–phonon coupling? Is the analytic continuum approximation adequate for predicting the properties of Davydov solitons in the case of anisotropic exciton-phonon interaction? The positive answers to the first three questions support the plausibility of Davydov solitons as a physical mechanism employed in the evolution of protein function through gradual steps favored by natural selection. The partially negative answer to the last question highlights the necessity of combining both computational and analytic approaches for studying the effects of lattice discreteness on the quantum transport of energy in proteins.

2. Computational study

2.1. Model parameters

The solitons described here are supported by the system of generalized Davydov equations (1) and (2) for a wide range of the biophysical parameters characterizing the protein α-helix [6, 17–24, 30–32, 37, 42]. In order to compare the results in this present work with those reported in previous studies, we have fixed the model parameters as follows: spring constant of the hydrogen bonds in the lattice $w = 13$ N/m [43], nonlinear exciton–phonon coupling parameter $\bar{\chi} = 35$ pN [6], uniform mass of amino acid residues $M = 1.9 \times 10^{-25}$ kg [24], and uniform amide I dipole–dipole coupling energy $J = 0.155$ zJ [44].

The solitons were produced in the absence of initial phonon dressing of the applied amide I energy pulses. Thus, the initial state at $t = 0$ of the lattice of hydrogen bonds was considered to be unperturbed, $b_n(0) = 0$ and $\frac{d}{dt} b_n(0) = 0$. Therefore, all of the energy supplied to the protein α-helix is due to a fixed non-zero initial exciton distribution $a_n(0)$ with $Q \geq 1$. To furnish a sufficient arena for phase modulation through phase parameter $\Delta\omega$, individual Gaussian pulses of amide I energy were spread over 7 peptide groups with quantum probability amplitudes a_n given by

$$\{A_3 e^{-\imath 3\Delta\omega}, A_2 e^{-\imath 2\Delta\omega}, A_1 e^{-\imath 1\Delta\omega}, A_0 e^{\imath 0\Delta\omega}, A_1 e^{+\imath 1\Delta\omega}, A_2 e^{+\imath 2\Delta\omega}, A_3 e^{+\imath 3\Delta\omega}\} \tag{3}$$

where $A_0 = \sqrt{0.286}$, $A_1 = \sqrt{0.222}$, $A_2 = \sqrt{0.105}$ and $A_3 = \sqrt{0.03}$.

Denoting the longitudinal axis of the α-helix spine by x, we can express the initial discrete distribution of exciton quantum probability amplitudes centered at x_0 as

$$a(x) = \sum_{j=-3}^{3} \frac{1}{\sqrt{r}} A_{|j|} e^{\imath j\Delta\omega} \left[\Theta\left(\frac{x-x_0}{r} - j + \frac{1}{2}\right) - \Theta\left(\frac{x-x_0}{r} - j - \frac{1}{2}\right) \right] \tag{4}$$

where $\Theta(x) = \frac{d}{dx} \max\{x, 0\}$ is the Heaviside step function and $r = 0.45$ nm is the distance between neighboring peptide groups along the spine. This initial exciton state is normalized

$$\int_{-\infty}^{\infty} |a(x)|^2 \, dx = A_0^2 + 2\left(A_1^2 + A_2^2 + A_3^2\right) = 1. \tag{5}$$

Application of a Fourier transform determines the exciton wavefunction in wavenumber basis k as

$$a(k) = \sqrt{\frac{2}{k^2 \pi r}} \sin\left(\frac{kr}{2}\right) e^{-\imath k x_0} \sum_{j=-3}^{3} A_{|j|} e^{\imath j(kr - \Delta\omega)}. \tag{6}$$

The wavenumber quantum probability distribution is

$$|a(k)|^2 = \frac{8 \sin^2\left(\frac{kr}{2}\right)}{k^2 \pi r} \left\{ \frac{A_0}{2} + \sum_{j=1}^{3} A_j \cos\left[j\left(kr - \Delta\omega\right)\right] \right\}^2 \tag{7}$$

with corresponding expectation value

$$\langle \hat{k} \rangle = \int_{-\infty}^{\infty} |a(k)|^2 \, k \, dk = \frac{2 \sin(\Delta\omega)}{r} \left(A_0 A_1 + A_1 A_2 + A_2 A_3\right). \tag{8}$$

Due to the initial unperturbed state of the phonon lattice, there is no phonon dressing of the exciton at $t = 0$, namely $\langle \Psi(0) | \hat{H}_{\mathrm{ph}} | \Psi(0) \rangle = 0$ and $\langle \Psi(0) | \hat{H}_{\mathrm{int}} | \Psi(0) \rangle = 0$, where the phonon Hamiltonian $\hat{H}_{\mathrm{ph}}$ and the exciton-phonon interaction Hamiltonian $\hat{H}_{\mathrm{int}}$ are given by [1]

$$\hat{H}_{\mathrm{ph}} = \frac{1}{2} \sum_n \left[\frac{\hat{p}_n^2}{M_n} + w\left(\hat{u}_{n+1} - \hat{u}_n\right)^2 \right], \tag{9}$$

$$\hat{H}_{\mathrm{int}} = \chi \sum_n \left(\hat{u}_{n+1} + (\xi - 1)\hat{u}_n - \xi\hat{u}_{n-1}\right) \hat{a}_n^\dagger \hat{a}_n, \tag{10}$$

$\hat{a}_n^\dagger$ and $\hat{a}_n$ are the boson creation and annihilation operators for the amide I excitons, $\hat{p}_n$ is the momentum operator and $\hat{u}_n$ is the displacement operator from the equilibrium position of the nth peptide group, and $|\Psi(0)\rangle$ is the initial state at $t = 0$ of the generalized ansatz state vector [29]

$$|\Psi(t)\rangle = |\psi_{\mathrm{ex}}(t)\rangle |\psi_{\mathrm{ph}}(t)\rangle \tag{11}$$

3

comprised of a Hartree approximate eigenstate for the excitons [33, 45–47]

$$|\psi_{\text{ex}}(t)\rangle = \frac{1}{\sqrt{Q!}} \left[\sum_n a_n(t) \hat{a}_n^\dagger \right]^Q |0_{\text{ex}}\rangle \qquad (12)$$

and a Glauber coherent phonon state for the lattice [33, 48, 49]

$$|\psi_{\text{ph}}(t)\rangle = e^{-\frac{i}{\hbar} \sum_j (b_j(t)\hat{p}_j - c_j(t)\hat{u}_j)} |0_{\text{ph}}\rangle. \qquad (13)$$

Because the total energy of the composite system is conserved during temporal evolution according to the Schrödinger equation, the soliton energy could be calculated from the initial expectation value of the exciton Hamiltonian

$$\hat{H}_{\text{ex}} = \sum_n \left[-J_{n+1} \hat{a}_n^\dagger \hat{a}_{n+1} - J_n \hat{a}_n^\dagger \hat{a}_{n-1} \right]. \qquad (14)$$

After setting all dipole–dipole coupling energies to be the same $J_n = J$, we obtain

$$\langle \Psi(0)|\hat{H}_{\text{ex}}|\Psi(0)\rangle = -QJ \sum_n \left[a_n^*(0) a_{n+1}(0) + a_n(0) a_{n+1}^*(0) \right]$$
$$= -4QJ \cos(\Delta\omega)(A_0 A_1 + A_1 A_2 + A_2 A_3). \qquad (15)$$

In the simulations with two amide I energy quanta ($Q = 2$), the exciton probability amplitudes of individual solitons (3) were multiplied by a factor of $\sqrt{\frac{1}{Q}}$ for two colliding single solitons or by a factor of $\sqrt{\frac{2}{Q}}$ for a single double soliton.

2.2. Effect of phase-modulation on single solitons

Extensive previous research with reflective boundary conditions has shown that in-phase Gaussian pulses of amide I energy generate moving Davydov solitons only when applied at one of the two ends of a protein α-helix, whereas the same pulses produce pinned solitons in the interior of the α-helix [1, 6, 37]. Because the biological function of proteins in living matter may require delivery and transport of energy irrespective of the application site, we have explored the possibility of utilizing phase-modulation to launch moving solitons in the interior of protein α-helices.

To investigate numerically how phase-modulation $\Delta\omega \in [-\pi, \pi]$ affects the velocity of generated Davydov solitons, we have applied Gaussian pulses of amide I energy centered at the peptide group $n = 10$ of a protein α-helix spine comprised of $n_{\text{max}} = 40$ peptide groups. For single solitons, a single quantum of amide I energy ($Q = 1$) was used.

For completely isotropic exciton–phonon interaction $\xi = 1$, in the absence of phase modulation ($\Delta\omega = 0$) the generated soliton remained pinned at the place of origin (Fig. 1a, Video 1). In the presence of positive phase modulation ($0 < \Delta\omega \le \frac{\pi}{2}$), the soliton moves to the right (Fig. 1b-d, Videos 2-3), whereas for negative phase modulation ($-\frac{\pi}{2} \le \Delta\omega < 0$), the soliton moves to the left (Fig. 2a-c). At $\Delta\omega = \pm\pi$, the soliton appears to be unstable and quickly disintegrates (Fig. 2d, Video 4).

The results of the simulations were qualitatively similar to those for completely anisotropic exciton–phonon interaction $\xi = 0$. In the absence of phase modulation ($\Delta\omega = 0$), the generated soliton remained pinned at the place of origin (Fig. 3a). In the presence of positive phase modulation ($0 < \Delta\omega < \frac{\pi}{2}$), the soliton moves to the right (Fig. 3b-c), whereas for negative phase modulation ($-\frac{\pi}{2} < \Delta\omega < 0$), the soliton moves to the left (Fig. 4a-b). Crucially, in this case the soliton instability is already pronounced at $\Delta\omega = \pm\frac{\pi}{2}$ (Figs. 3d and 4c), and the soliton also quickly disintegrates at $\Delta\omega = \pm\pi$ (Fig. 4d).

Because the total energy of the composite system is conserved throughout the simulations, it is equal to the initial exciton energy (15) applied to the protein α-helix. For $\Delta\omega \in [0, \pm\frac{\pi}{2})$ the total energy stays negative, which is consistent with the observed persistence of the Davydov solitons as launched. However, when the phase modulation is $\Delta\omega \in (\pm\frac{\pi}{2}, \pm\pi]$, the total energy becomes positive and this facilitates dispersal of the exciton quantum probability amplitudes without any soliton formation.
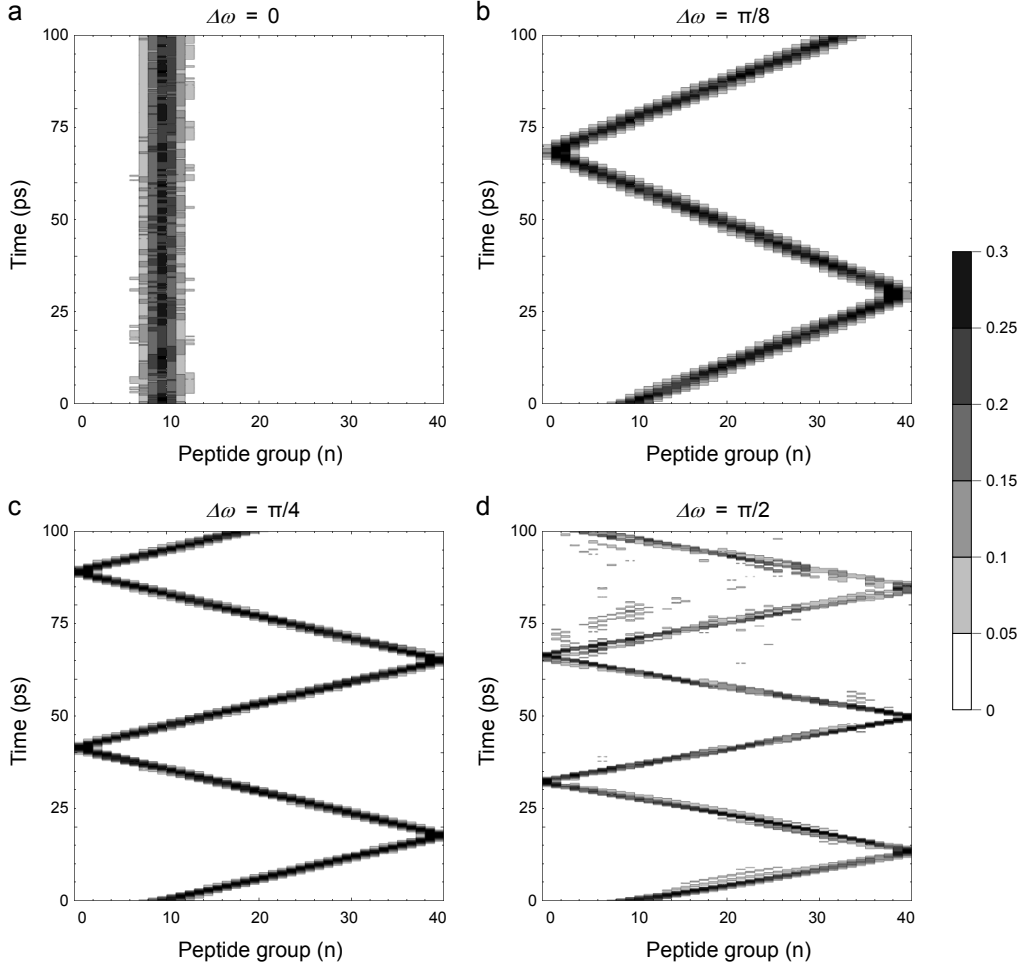
Figure 1: Single soliton dynamics for $Q = 1$ and $\xi = 1$, visualized in a contour plot of the amide I exciton expectation value $Q|a_n|^2$. The applied energy pulse is centered at the peptide group $n = 10$ of a protein α-helix spine comprised of $n_{\max} = 40$ peptide groups. In the absence of phase modulation $\Delta\omega = 0$ (a), the soliton is pinned. In the presence of positive phase modulation, $\Delta\omega = \frac{\pi}{8}$ (b), $\Delta\omega = \frac{\pi}{4}$ (c) or $\Delta\omega = \frac{\pi}{2}$ (d), the soliton moves to the right.

Previous analytical models [9, 10, 13, 33] of an α-helix spine have determined the effective mass of a single exciton

$$m_{\text{ex}} = \frac{\hbar^2}{2r^2 J} \tag{16}$$

and the effective mass of a single Davydov soliton [13]

$$m_{\text{sol}} = m_{\text{ex}} \left(1 + \frac{8M\chi^4}{3w^3\hbar^2} \right) \tag{17}$$

From (8) and (17), the soliton velocity can be predicted

$$v = \frac{\hbar\langle\hat{k}\rangle}{m_{\text{sol}}} = \frac{4rJ\left(A_0 A_1 + A_1 A_2 + A_2 A_3\right)}{\hbar + \frac{128M\bar{\chi}^4}{3w^3\hbar(1+\xi)^4}} \sin\left(\Delta\omega\right) \tag{18}$$

The velocity of single solitons ($Q = 1$) observed in the simulations was close to the predicted velocity (18) for $\xi = 1$ when $\Delta\omega < \frac{\pi}{4}$ and for $\xi = 0$ when $\Delta\omega < \frac{7}{16}\pi$ (Fig. 5). Due to larger effective mass, the solitons
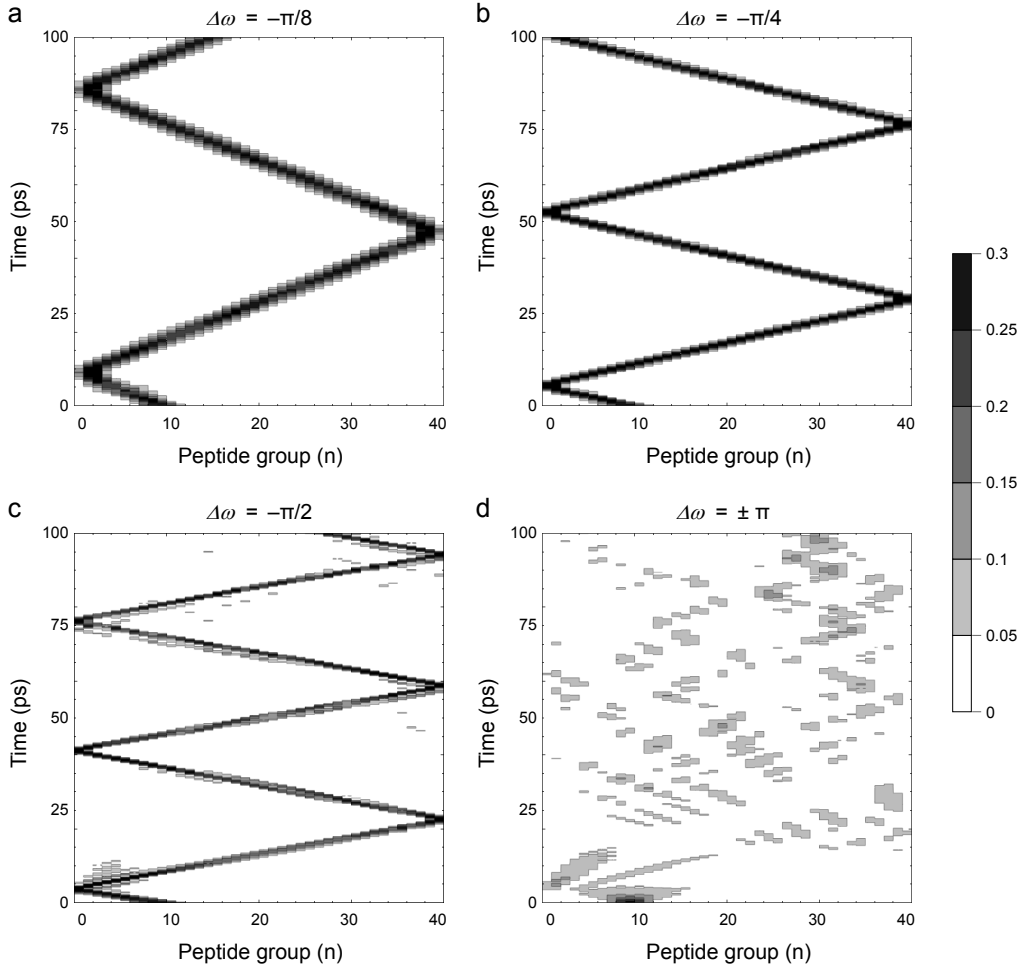
Figure 2: Single soliton dynamics for $Q = 1$ and $\xi = 1$, visualized in a contour plot of the amide I exciton expectation value $Q|a_n|^2$. The applied energy pulse is centered at the peptide group $n = 10$ of a protein α-helix spine comprised of $n_{\max} = 40$ peptide groups. In the presence of negative phase modulation, $\Delta\omega = -\frac{\pi}{8}$ (a), $\Delta\omega = -\frac{\pi}{4}$ (b) or $\Delta\omega = -\frac{\pi}{2}$ (c), the soliton moves to the left. At $\Delta\omega = \pm\pi$ (d), the soliton is unstable and quickly disintegrates.

for $\xi = 0$ were on average 25% slower than those for $\xi = 1$. Noteworthy, the heavier mass and lower velocity were not correlated with greater soliton stability. Instead, the generated solitons were unstable for $\xi = 0$ when the phase modulation was $\Delta\omega \in [\frac{7}{16}\pi, \frac{\pi}{2}]$ and exhibited features of disintegration by the end of the 100 ps simulation period (Figs. 3d, 4c and 5b).

Collectively, the above results indicate that moving Davydov solitons can be launched through phase-modulated Gaussian pulses of amide I energy even in the absence of initial phonon dressing. Thus, in the process of evolutionary design and optimization of protein function, it is physically plausible that different biomolecular catalysts such as protein master proteins are able to deliver chemical energy to protein α-helical motifs where this energy is transported and utilized through a soliton mechanism operating at biologically relevant timescale of tens of picoseconds.

2.3. Effect of phase-modulation on double solitons

To further investigate the resulting quantum dynamics in the presence of two amide I quanta ($Q = 2$), we have generated double Davydov solitons for different values of the phase-modulation parameter $\Delta\omega \in [0, \frac{\pi}{2}]$. For completely isotropic exciton–phonon interaction $\xi = 1$, the non-zero phase modulation of the initial
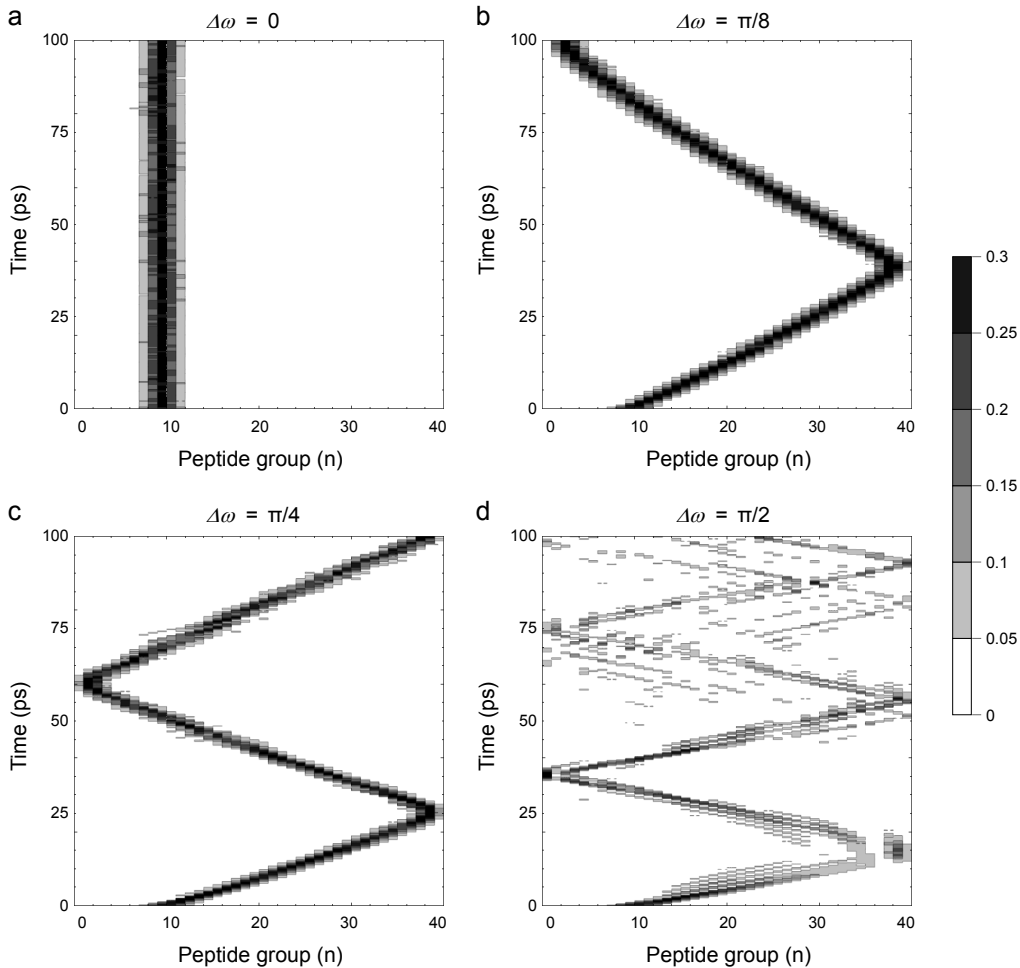
Figure 3: Single soliton dynamics for $Q = 1$ and $\xi = 0$, visualized in a contour plot of the amide I exciton expectation value $Q|a_n|^2$. The applied energy pulse is centered at the peptide group $n = 10$ of a protein α-helix spine comprised of $n_{\max} = 40$ peptide groups. In the absence of phase modulation $\Delta\omega = 0$ (a), the soliton is pinned. In the presence of positive phase modulation, $\Delta\omega = \frac{\pi}{8}$ (b) or $\Delta\omega = \frac{\pi}{4}$ (c) the soliton moves to the right. For $\Delta\omega = \frac{\pi}{2}$ (d), the soliton is unstable.

amide I energy Gaussian distribution was able to launch moving solitons in the interior of the protein α-helix (Fig. 6b-d). For completely anisotropic exciton–phonon interaction $\xi = 0$, however, the solitons remained pinned despite the presence of significant phase modulation $\Delta\omega \in [0, \frac{3}{8}\pi)$ (Fig. 7b-c). In the range $\Delta\omega \in [\frac{\pi}{4}, \frac{3}{8}\pi)$, the pinned solitons wobbled around their place of origin, whereas in the range $\Delta\omega \in [\frac{3}{8}\pi, \frac{\pi}{2}]$ the solitons were unstable and disintegrated. The theoretical prediction of soliton velocity based on double effective soliton mass was quantitatively close to the observed velocity for $\xi = 1$ (Fig. 8a), but it was inadequate to capture the qualitative transition towards soliton pinning for $\xi = 0$ (Fig. 8b).

Again collectively, the above results indicate that theoretically derived analytic results for the soliton velocity based on effective soliton mass might be applicable only for a narrow window of the physical parameters in which moving soliton solutions exist. Extensive previous computational research with the same generalized Davydov Hamiltonian $\hat{H} = \hat{H}_{\mathrm{ex}} + \hat{H}_{\mathrm{ph}} + \hat{H}_{\mathrm{int}}$ [1, 6, 37, 50] has established the existence of two different thresholds for the nonlinear coupling parameter χ: a lower threshold for which the self-trapping mechanism is strong enough to prevent the soliton from dispersing and an upper threshold for which the self-trapping is so strong that the soliton remains pinned at the place of its origin [6]. Because the number of amide I quanta Q appears as a multiplicative factor in front of χ in the second Davydov equation (2), its
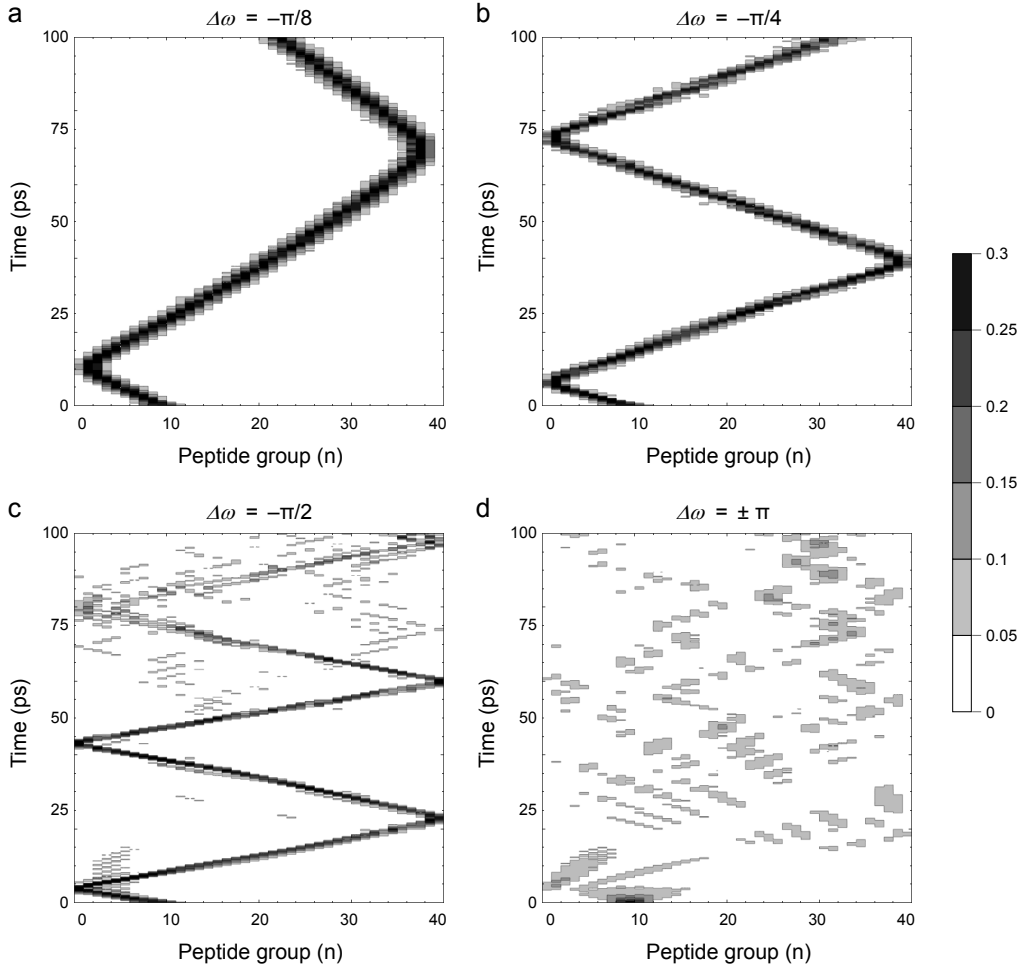
Figure 4: Single soliton dynamics for $Q = 1$ and $\xi = 0$, visualized in a contour plot of the amide I exciton expectation value $Q|a_n|^2$. The applied energy pulse is centered at the peptide group $n = 10$ of a protein α-helix spine comprised of $n_{\max} = 40$ peptide groups. In the presence of negative phase modulation, $\Delta\omega = -\frac{\pi}{8}$ (a) or $\Delta\omega = -\frac{\pi}{4}$ (b), the soliton moves to the left. For $\Delta\omega = -\frac{\pi}{2}$ (c) the soliton is unstable, and at $\Delta\omega = \pm\pi$ (d) it quickly disintegrates.

main effect is to strengthen the self-trapping mechanism thereby shifting the threshold for soliton formation or pinning towards lower values of χ. As a result, protein structures with low nonlinear exciton–phonon coupling might be also conductive for solitons at the expense of increasing the number of amide I energy quanta (Fig. 9). This would be particularly important at early stages of protein function optimization, namely a novel protein function could be initially supported by high energy flux even in the case of low nonlinear exciton–phonon coupling and then gradually the efficiency could be increased by decreasing the energy flux as the soliton stability is assisted by strengthened nonlinear exciton–phonon coupling.

2.4. Two-soliton collisions

Having demonstrated that the phase modulation is a robust physical mechanism that could launch moving single solitons in the interior of the α-helix, we have also explored how the generated solitons interact when they collide with each other. For simulating soliton collisions, we have used two quanta of amide I energy ($Q = 2$) and launched two phase-modulated single solitons from the two ends of the α-helix thereby ensuring maximal distance between the starting soliton positions. The soliton launched from the left was used as a probe with fixed phase-modulation $\Delta\omega_1 = \frac{\pi}{8}$. The other soliton launched from the right was then tested for
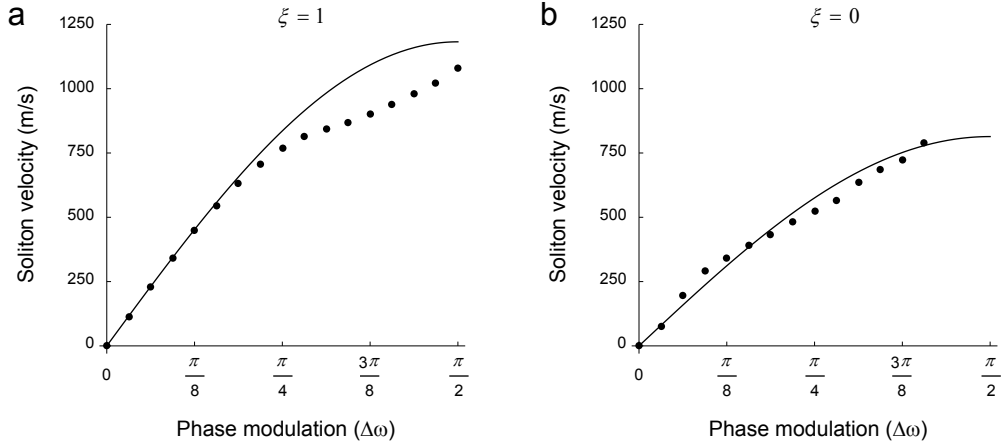
Figure 5: The velocity of single Davydov solitons for $Q = 1$ plotted as a function of the phase modulation parameter $\Delta\omega$. Solitons move faster for $\xi = 1$ (a) compared with $\xi = 0$ (b). The theoretical prediction of soliton velocity based on effective soliton mass (solid line) fits well the observed velocity (black circles) for $\xi = 1$ when $\Delta\omega < \frac{\pi}{4}$ and for $\xi = 0$ when $\Delta\omega < \frac{7}{16}\pi$. The generated solitons are unstable for $\xi = 0$ when $\Delta\omega \in [\frac{7}{16}\pi, \frac{\pi}{2}]$.

different values of phase modulation $\Delta\omega_2 \in \left\{0, -\frac{\pi}{8}, -\frac{\pi}{4}, -\frac{\pi}{2}\right\}$. Because the negative sign of $\Delta\omega_2$ indicates only the reversed direction of motion, whereas the absolute value $|\Delta\omega_2|$ affects the soliton speed and stability, we will report the dynamic consequences of increasing the latter.

For $\xi = 1$, the solitons exhibited constructive or destructive quantum interference at the collision sites exemplifying the quantum nature of the Davydov quasiparticles (Fig. 10). The colliding solitons were also able to preserve their shape and velocity after the collisions provided that the phase modulation of the second soliton is in the range $|\Delta\omega_2| \in [0, \frac{\pi}{4}]$ (Fig. 10a-c). When the phase modulation of the second soliton is larger, $|\Delta\omega_2| = \frac{\pi}{2}$, the discreteness of the protein lattice leads to much more pronounced leakage of exciton quantum probability amplitudes, which tends to equalize the velocities of the two solitons recovered after each collision (Fig. 10d).

For $\xi = 0$, the solitons were more massive and moved with slower velocities (Fig. 11). In the case of destructive quantum interference, e.g. when $|\Delta\omega_2| = 0$, the solitons passed through each other preserving their original shape and velocity (Fig. 11a). The occurrence of constructive quantum interference at the collision sites, however, lead to formation of pinned solitons, e.g. when $|\Delta\omega_2| \in \left\{\frac{\pi}{8}, \frac{\pi}{4}\right\}$ (Fig. 11b-c). Increasing the phase modulation of the second soliton to $|\Delta\omega_2| = \frac{\pi}{2}$ exhibited the instability already observed in the single soliton case, which was further accelerated by the soliton collisions (Fig. 11d).

Taken in their entirety, the above results support the possibility that quantum interference could have important functional consequences within living systems [1]. Indeed, constructive quantum interference might play an important role in focusing transported energy for its utilization at protein active sites. Alternatively, destructive quantum interference might be useful to avoid accidental absorption of transported energy at unfavorable protein sites. Local modification of the isotropy of exciton–phonon interaction ξ through structural changes of the physical distances between peptide groups of sequential amino acids may also optimize certain protein active sites to retain the delivered energy in place through pinned solitons [1].

3. Discussion

Proteins sustain essential life mechanisms through catalysis of biochemical processes in living organisms. Because the protein function involves physical work, it can only be performed at the expense of free energy released by biochemical reactions such as ATP hydrolysis. To investigate deeper the quantum transport of energy inside protein α-helices, we have explored the generalized Davydov model that describes each α-helix spine as a lattice of hydrogen bonded peptide groups. We have performed numerical simulations of the
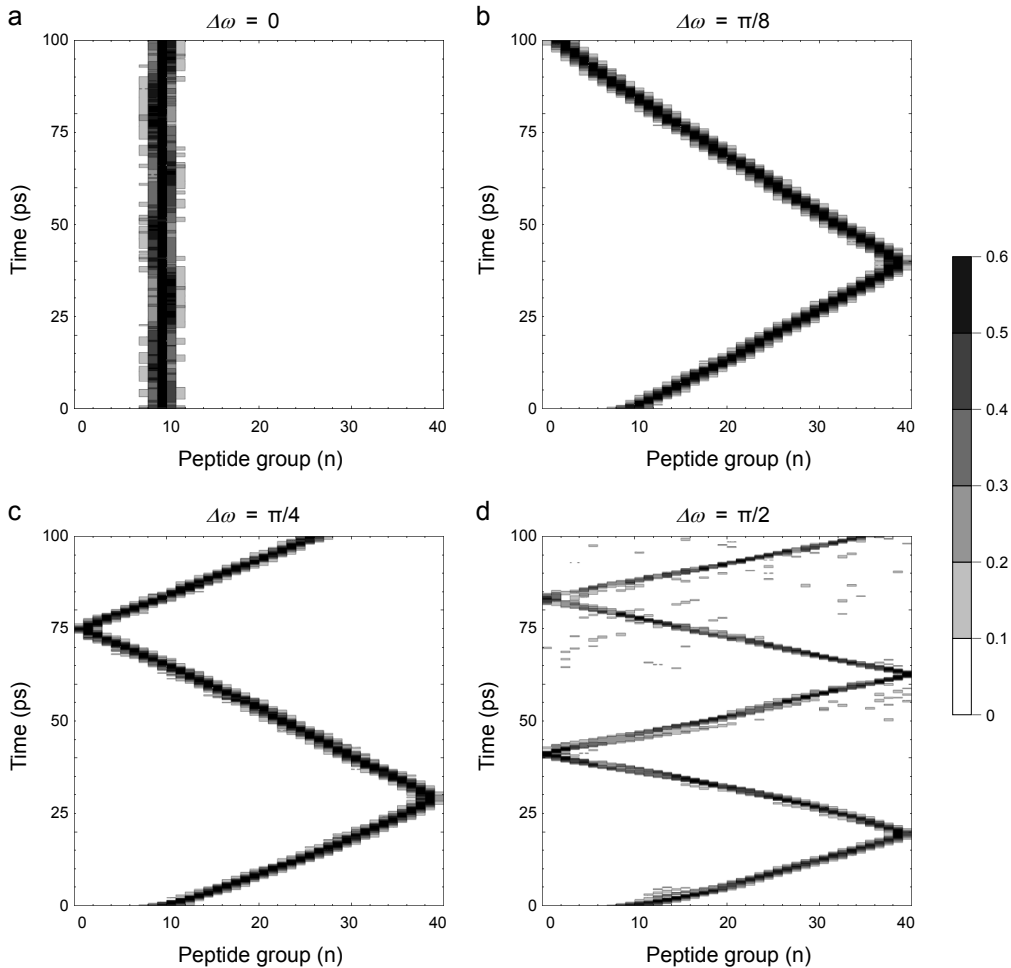
Figure 6: Double soliton dynamics for $Q = 2$ and $\xi = 1$, visualized in a contour plot of the amide I exciton expectation value $Q|a_n|^2$. The applied energy pulse is centered at the peptide group $n = 10$ of a protein α-helix spine comprised of $n_{\max} = 40$ peptide groups. In the absence of phase modulation $\Delta\omega = 0$ (a), the soliton is pinned. In the presence of positive phase modulation, $\Delta\omega = \frac{\pi}{8}$ (b), $\Delta\omega = \frac{\pi}{4}$ (c) or $\Delta\omega = \frac{\pi}{2}$ (d), the soliton moves to the right.

quantum dynamics of a protein α-helix spine for Gaussian pulses of amide I energy applied over a region of 7 peptide groups and have confirmed the generation of either moving or stationary Davydov solitons depending on the degree of phase modulation of the initial pulses.

Previous analytical work by Davydov and colleagues [7–15, 17–23, 42, 51] has been successful in deriving important results in regard to the optimal shape of the solitons, as well as their energy, effective mass and velocity. The analytic method (presented in details in Appendix A), however, relies upon a number of essential assumptions, satisfaction of which may be questionably determinable in the historical early stages of life evolution. For example, it is unlikely that proteins would have been able to deliver energy pulses tailored precisely to the form of a sech-squared shape, or to supply an exact initial phonon dressing for soliton production. Similarly, elaborate mechanisms for control of soliton direction and speed may have been lacking in prebiotic systems. Furthermore, protein α-helical secondary structure is sensitive to environmental conditions including pH, and local hydrophobicity of the environment [52–54], which would impact the strength of the nonlinear exciton–phonon coupling χ, as well as the efficacy of the soliton self-trapping mechanism. In addition, the existence of a threshold for soliton formation appears to suggest that the transport of energy by solitons is an all-or-none phenomenon for which natural selection is challenged
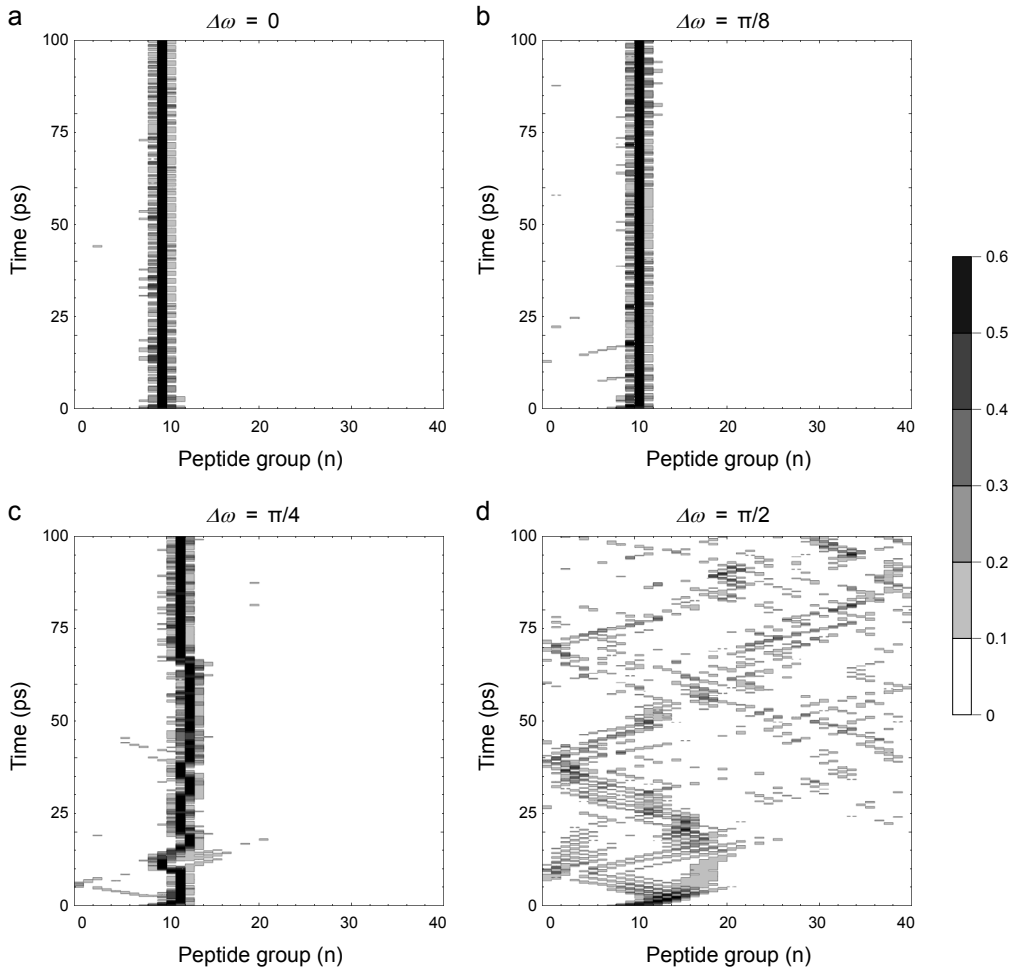
Figure 7: Double soliton dynamics for $Q = 2$ and $\xi = 0$, visualized in a contour plot of the amide I exciton expectation value $Q|a_n|^2$. The applied energy pulse is centered at the peptide group $n = 10$ of a protein α-helix spine comprised of $n_{\max} = 40$ peptide groups. The soliton remains pinned despite any phase modulation, $\Delta\omega = 0$ (a), $\Delta\omega = \frac{\pi}{8}$ (b) or $\Delta\omega = \frac{\pi}{4}$ (c). When the phase modulation reaches $\Delta\omega = \frac{\pi}{2}$ (d), the soliton disintegrates instead of being set in motion.

to provide gradual steps of improvement in the evolutionary history. Here, we have been able to address all of these problems in a physically rigorous manner supported through extensive computational simulations.

Firstly, we have established that initial phonon dressing is not absolutely required, and applied amide I energy pulses could have Gaussian shape supporting the generated solitary waves for a lifetime of tens of picoseconds. This timescale is biologically relevant because the solitons are able to traverse the whole extent of an average protein α-helix and deliver the transported energy for use at a specific protein active site. Thus, the analytic sech-squared soliton solution is to be considered as an idealized mathematical entity whose possibly infinite lifetime does not need to be attained. Instead, biological functionality could be achieved by proteins with energy pulses whose Gaussian shape suffices to support the self-trapping mechanism for only a finite lifetime of tens of picoseconds.

Secondly, we have shown that moving solitons can be launched at any site in the protein through phase modulation of the applied amide I energy Gaussian pulse. Phase modulation should occur naturally since the ATP hydrolysis sites would have different distances to different locations in nearby protein α-helices and quantum paths with different lengths would accumulate different phases according to Feynman's path integral formalism [55–58]. Therefore, the relative orientation and distance between an ATP hydrolysis site
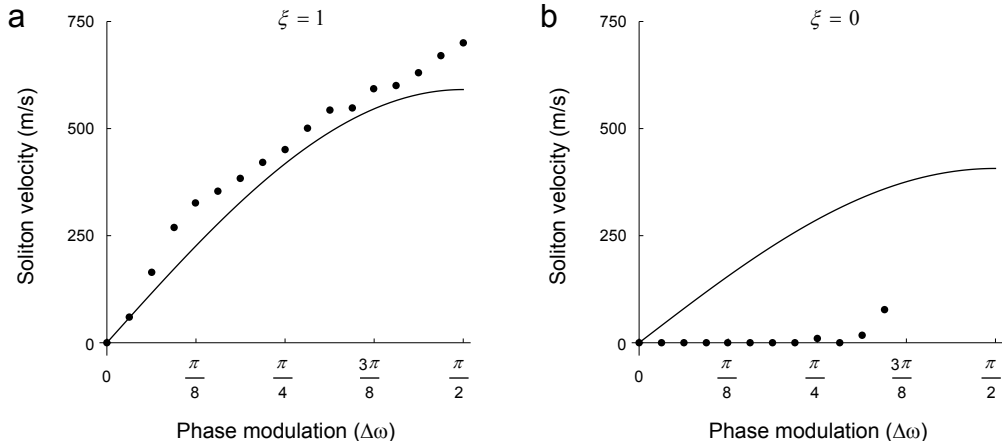
Figure 8: The velocity of double Davydov solitons for $Q = 2$ plotted as a function of the phase modulation parameter $\Delta\omega$. Solitons are able to move for $\xi = 1$ (a) as opposed to being pinned for $\xi = 0$ (b). The theoretical prediction of soliton velocity based on double effective soliton mass (solid line) is close to the observed velocity (black circles) for $\xi = 1$ but it is inadequate to capture the soliton pinning for $\xi = 0$. The generated solitons are unstable for $\xi = 0$ when $\Delta\omega \in [\frac{7}{16}\pi, \frac{\pi}{2}]$.

and a receptive protein α-helix, should be sufficient for proteins to be able to control the direction and velocity of generated solitons.

Thirdly, we have demonstrated that low values of the nonlinear exciton–phonon coupling χ, that are otherwise below the threshold for soliton formation could be compensated by an increased number of amide I quanta in the energy pulses. Thus, in environments that destabilize the α-helical secondary structure, protein functionality through soliton transport could have been achieved at the expense of higher energy fluxes. At later evolutionary stages, when the living systems have a better control of the relevant protein environment, thereby increasing χ, the same functionality would be attained with fewer amide I energy quanta.

Fourthly, we have brought into focus the existence of transient solutions that may look like solitary waves, only for a finite period of time after which the amide I exciton quantum probability amplitudes disperse. Referring to such transient solutions as solitons is in line with Davydov's own statement that "for describing real systems even unstable solitary waves can be significant if their lifetime is long in comparison with the time during which the phenomenon under study takes place" [13]. For Davydov, the notion of soliton (that is, as a quasiparticle) had to be understood in a wider meaning as describing "any autolocalized excitations propagating without significant change in their form and velocity owing to the dynamical balance between nonlinearity and dispersion" [13]. In this general context, the most important dynamic quantity becomes the soliton lifetime, which can be operationally defined as the time for which the localized exciton wave loses e.g. half of its initial amplitude. Because the soliton lifetime has a continuous range of values, it is subject to gradual improvement through natural selection as mandated by evolutionary theory. This explains how proteins might have indeed evolved mechanisms for transport of energy through Davydov solitons.

Although the presented results illustrate the rich variety of physical phenomena contained in the Davydov model, they are inevitably constrained by our choice of biophysical parameters and the decision to focus on the dynamics of a single protein α-helix spine. Quantum chemical *ab initio* computation of the protein material properties utilizing recent developments in density functional theory (DFT) [59, 60] is certainly desirable as it may help revise the range of the biophysical parameters appearing in the Davydov model. Extension of the model to a full protein α-helix with three spines [51, 61] or inclusion of environmental interactions such as the presence of external electromagnetic fields [42] may further inform our understanding of how proteins function.

One promising line for future research would be to perform all-atom molecular dynamics (MD) simulations, which could demonstrate soliton emergence and propagation in real α-helical proteins. Use of atomically detailed force fields, in which interatomic interactions are considered explicitly [62, 63], would
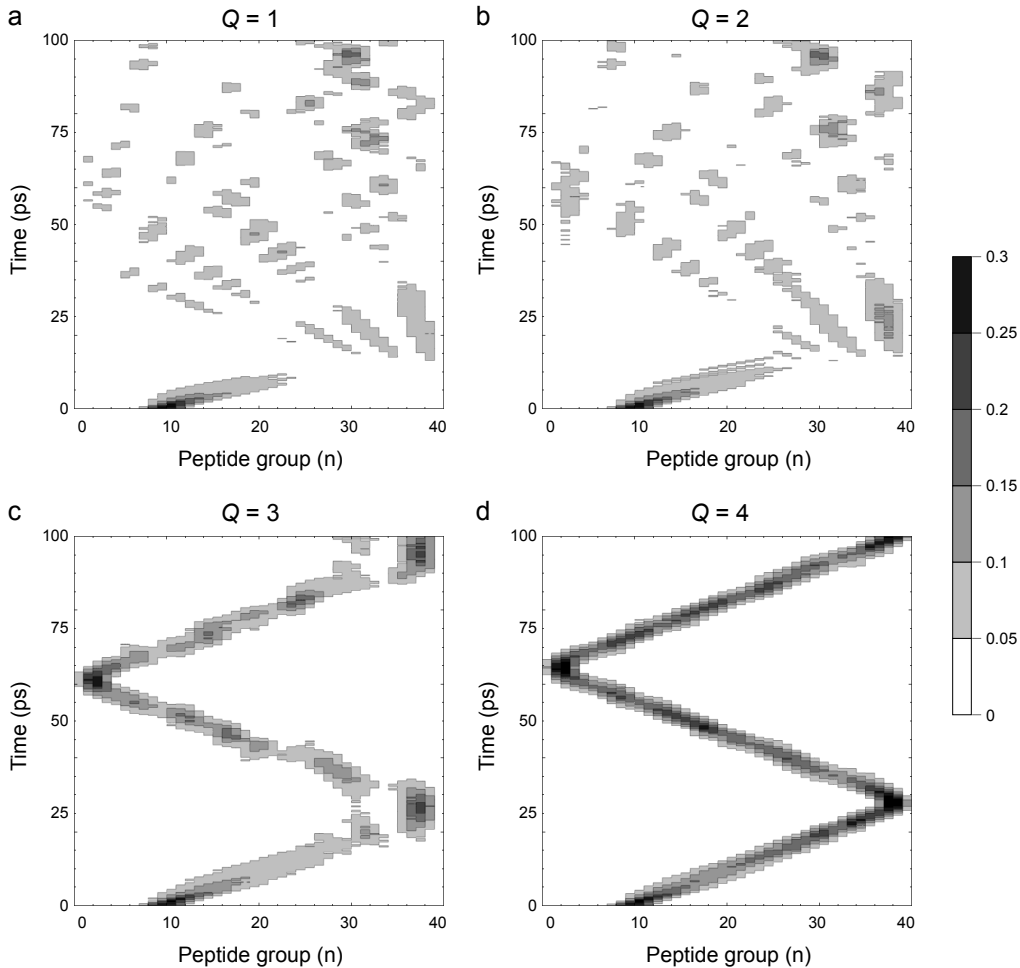
12

Figure 9: Launching of a phase-modulated $\Delta\omega = \frac{\pi}{8}$ Davydov soliton for $\xi = 1$ in the interior of a protein α-helix with low value of the nonlinear exciton–phonon coupling parameter $\bar{\chi} = 15$ pN, visualized through $|a_n|^2$. Increasing the number of amide I excitons to $Q \geq 3$ is able to strengthen the self-trapping mechanism thereby shifting the threshold of $\bar{\chi}$ for soliton formation: $Q = 1$ (a), $Q = 2$ (b), $Q = 3$ (c) and $Q = 4$ (d).

allow distortion of a selected C=O bond followed by running a number of protein simulations to gather sufficient statistics on the dynamics of hydrogen bonds supporting the α-helix structure.

Another promising line of research is to use a generalized discrete nonlinear Schrödinger equation (DNLSE) arising from a C_α-trace-based energy function to study topological solitons involved in protein folding [64–67]. Using their united-residue (UNRES) force field simulations, with respect to the staphylococcal protein A, Niemi and coworkers already did substantial work on soliton propagation and energy transport in proteins at a coarse-grained level [68–70]. Although the topological solitons there are manifested as perturbation of geometric chain geometry-symmetry, and not hydrogen-bond network (involving C=O distortions), the coarse-grained description is expected to be intimately related to the asymmetric three-spine Davydov soliton, which spontaneously breaks the local translational and helical symmetries [21]. In particular, asymmetric stretching, or contraction of the hydrogen bonds in the three parallel α-helix spines will induce a topological kink in the protein, and conversely, the presence of a topological kink will inevitably distort the hydrogen bonds in the protein α-helix spines. The free energy of kink formation in the coarse-grained molecular dynamics was observed to be ≈ 7 kcal/mol, which roughly corresponds to a double Davydov soliton with $Q = 2$ amide I quanta. Because the Davydov model is also mathematically
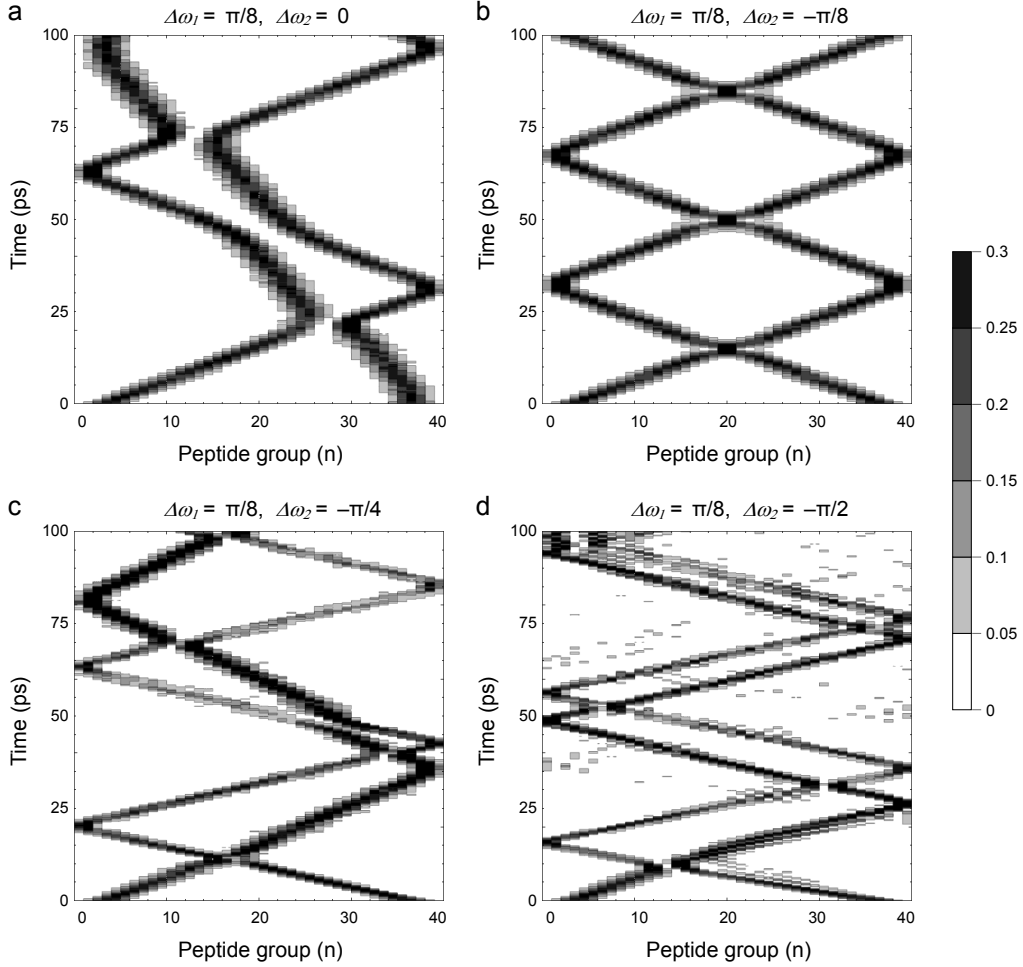
Figure 10: The quantum collision of two phase-modulated solitons for $\xi = 1$ launched from the two ends of a protein α-helix spine, carrying in total $Q = 2$ amide I excitons, visualized in a contour plot of $Q|a_n|^2$. Constructive or destructive quantum interference may occur at the collision sites. The phase modulation parameter of the soliton moving to the right is fixed to $\Delta\omega_1 = \frac{\pi}{8}$. The phase modulation parameter of the soliton moving to the left varies across different panels: $\Delta\omega_2 = 0$ (a), $\Delta\omega_2 = -\frac{\pi}{8}$ (b), $\Delta\omega_2 = -\frac{\pi}{4}$ (c) and $\Delta\omega_2 = -\frac{\pi}{2}$ (d).

based on DNLSE, our findings in regard to the effects of phase modulation on soliton velocity might be also applicable to protein folding, and thus we are not too far apart from the results reported in Ref. [70]. For example, in-phase pulses of energy are expected to produce stationary topological kinks in the protein structure, whereas phase-modulated pulses of energy are expected to produce traveling kinks that transport energy, and hence subserve the functionally important motions of proteins.

Conflict of interest

The authors declare that they have no conflict of interest.

Appendix A. Continuum approximation

The continuum approximation employs the mathematical transformations $f_n \rightarrow f(x,t)$ and $f_{n\pm1} \rightarrow \left[1 \pm r\frac{\partial}{\partial x} + \frac{r^2}{2}\frac{\partial^2}{\partial x^2}\right] f(x,t)$ in order to replace the set of discrete functions in the system of generalized
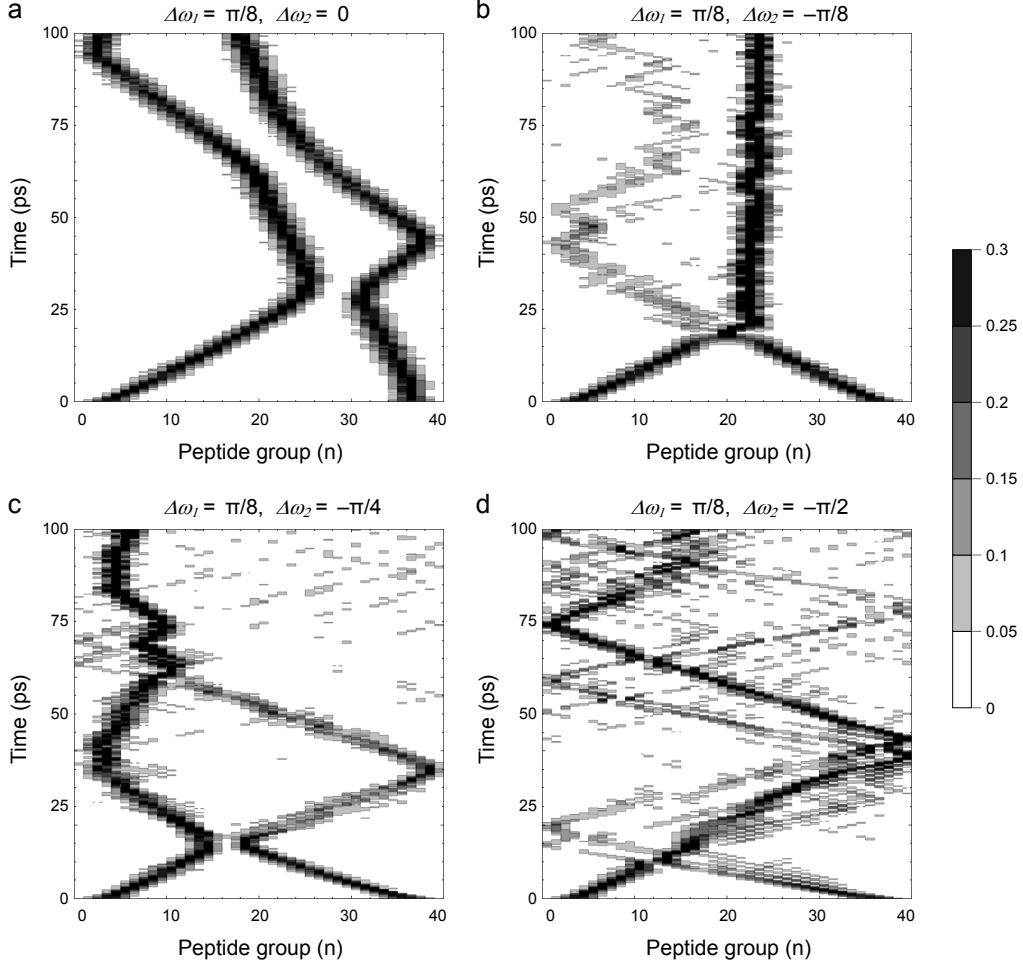
Figure 11: The quantum collision of two phase-modulated solitons for $\xi = 0$ launched from the two ends of a protein α-helix spine, carrying in total $Q = 2$ amide I excitons, visualized in a contour plot of $Q|a_n|^2$. Constructive or destructive quantum interference may occur at the collision sites. The phase modulation parameter of the soliton moving to the right is fixed to $\Delta\omega_1 = \frac{\pi}{8}$. The phase modulation parameter of the soliton moving to the left varies across different panels: $\Delta\omega_2 = 0$ (a), $\Delta\omega_2 = -\frac{\pi}{8}$ (b), $\Delta\omega_2 = -\frac{\pi}{4}$ (c) and $\Delta\omega_2 = -\frac{\pi}{2}$ (d).

Davydov equations (1) and (2) with corresponding continuous functions. The system of discrete ordinary differential equations (ODEs), then becomes a system of two partial differential equations (PDEs) in terms of the exciton distribution $a\,(x,t)$ and the phonon displacements $b\,(x,t)$. For ease of notation, we will leave the spatial and temporal dependence of $a\,(x,t)$ and $b\,(x,t)$ implicit

$$\imath\hbar\frac{\partial a}{\partial t} \;=\; -2Ja - Jr^2\frac{\partial^2 a}{\partial x^2} + \chi a\left[(1+\xi)\,r\frac{\partial b}{\partial x} + (1-\xi)\,\frac{r^2}{2}\frac{\partial^2 b}{\partial x^2}\right] \tag{A.1}$$

$$M\frac{\partial^2 b}{\partial t^2} \;=\; wr^2\frac{\partial^2 b}{\partial x^2} + Q\chi\left[(1+\xi)\,r\frac{\partial |a|^2}{\partial x} - (1-\xi)\,\frac{r^2}{2}\frac{\partial^2 |a|^2}{\partial x^2}\right] \tag{A.2}$$

Searching for a solution traveling at a constant speed v such that $\frac{\partial^2}{\partial t^2}b = v^2\frac{\partial^2}{\partial x^2}b$, we can rearrange (A.2) in the form

$$\frac{\partial^2 b}{\partial x^2} = -\frac{Q\chi}{wr}\frac{1}{(1-s^2)}\left[(1+\xi)\,\frac{\partial |a|^2}{\partial x} - (1-\xi)\,\frac{r}{2}\frac{\partial^2 |a|^2}{\partial x^2}\right] \tag{A.3}$$

15

where $s = \frac{v}{v_0}$ and $v_0 = r\sqrt{\frac{w}{M}}$ is the velocity of longitudinal sound waves in the chain of peptide groups [9, 13]. Integrating once with respect to x and setting the integration constant to zero gives

$$\frac{\partial b}{\partial x} = -\frac{Q\chi}{wr}\frac{1}{(1-s^2)}\left[(1+\xi)|a|^2 - (1-\xi)\frac{r}{2}\frac{\partial|a|^2}{\partial x}\right] \quad (A.4)$$

After substitution of (A.3) and (A.4) in (A.1), we obtain

$$i\hbar\frac{\partial a}{\partial t} = -2Ja - Jr^2\frac{\partial^2 a}{\partial x^2} - a\frac{Q\chi^2}{w(1-s^2)}\left[(1+\xi)^2|a|^2 - (1-\xi)^2\frac{r^2}{4}\frac{\partial^2|a|^2}{\partial x^2}\right] \quad (A.5)$$

If we consider the isotropic case $\xi = 1$, which was originally proposed by Davydov [9], we obtain the nonlinear Schrödinger equation (NLSE) [71, 72] in a standard form

$$\left[i\frac{\partial}{\partial t} + \alpha + \beta\frac{\partial^2}{\partial x^2} + \gamma|a|^2\right]a = 0 \quad (A.6)$$

with $\alpha = \frac{2J}{\hbar}$, $\beta = \frac{Jr^2}{\hbar}$ and $\gamma = \frac{4Q\chi^2}{\hbar w(1-s^2)}$. The analytic soliton solution centered at x_0 is

$$a(x,t) = \sqrt{\frac{2}{\gamma}}\mathrm{sech}\left[\sqrt{\frac{1}{\beta}}(x-x_0-vt)\right]\exp\left[i(\alpha+1)t + i\frac{v}{2\beta}\left(x-x_0-\frac{1}{2}vt\right)\right] \quad (A.7)$$

with corresponding sech-squared exciton probability distribution

$$|a(x,t)|^2 = \frac{2}{\gamma}\mathrm{sech}^2\left[\sqrt{\frac{1}{\beta}}(x-x_0-vt)\right] \quad (A.8)$$

Appendix B. Supplementary videos

Video 1. Quantum dynamics of a Davydov soliton carrying a single amide I exciton ($Q = 1$), simulated for 100 ps with completely isotropic exciton–phonon interaction $\xi = 1$, and visualized through $\mathrm{Re}(a_n)$ and $\mathrm{Im}(a_n)$ of the exciton quantum probability amplitudes. The applied amide I energy pulse is centered at the peptide group $n = 10$ of a protein α-helix spine comprised of $n_{\max} = 40$ peptide groups. In the absence of phase modulation $\Delta\omega = 0$, the soliton is pinned.

Video 2. The quantum dynamics of a Davydov soliton carrying a single amide I exciton ($Q = 1$), simulated for 100 ps with completely isotropic exciton–phonon interaction $\xi = 1$, and visualized through $\mathrm{Re}(a_n)$ and $\mathrm{Im}(a_n)$ of the exciton quantum probability amplitudes. The applied amide I energy pulse is centered at the peptide group $n = 10$ of a protein α-helix spine comprised of $n_{\max} = 40$ peptide groups. In the presence of phase modulation $\Delta\omega = \frac{\pi}{4}$, the soliton moves to the right.

Video 3. The quantum dynamics of a Davydov soliton carrying a single amide I exciton ($Q = 1$), simulated for 100 ps with completely isotropic exciton–phonon interaction $\xi = 1$, and visualized through $\mathrm{Re}(a_n)$ and $\mathrm{Im}(a_n)$ of the exciton quantum probability amplitudes. The applied amide I energy pulse is centered at the peptide group $n = 10$ of a protein α-helix spine comprised of $n_{\max} = 40$ peptide groups. In the presence of phase modulation $\Delta\omega = \frac{\pi}{2}$, the soliton moves faster to the right but starts to lose amplitude.

Video 4. The quantum dynamics of a Davydov soliton carrying a single amide I exciton ($Q = 1$), simulated for 100 ps with completely isotropic exciton–phonon interaction $\xi = 1$, and visualized through $\mathrm{Re}(a_n)$ and $\mathrm{Im}(a_n)$ of the exciton quantum probability amplitudes. The applied amide I energy pulse is centered at the peptide group $n = 10$ of a protein α-helix spine comprised of $n_{\max} = 40$ peptide groups. In the presence of phase modulation $\Delta\omega = \pi$, the soliton is unstable and quickly disintegrates.

References

[1] D. D. Georgiev, J. F. Glazebrook, Quantum transport and utilization of free energy in protein α-helices, Advances in Quantum Chemistry 82 (2020) in press. `doi:10.1016/bs.aiq.2020.02.001`.

[2] J. M. Scholtz, R. L. Baldwin, The mechanism of α-helix formation by peptides, Annual Review of Biophysics and Biomolecular Structure 21 (1) (1992) 95–118. `doi:10.1146/annurev.bb.21.060192.000523`.

[3] W. D. Kohn, C. T. Mant, R. S. Hodges, α-helical protein assembly motifs, Journal of Biological Chemistry 272 (5) (1997) 2583–2586. `doi:10.1074/jbc.272.5.2583`.

[4] B. Haimov, S. Srebnik, A closer look into the α-helix basin, Scientific Reports 6 (1) (2016) 38341. `doi:10.1038/srep38341`.

[5] L. Pauling, R. B. Corey, H. R. Branson, The structure of proteins: two hydrogen-bonded helical configurations of the polypeptide chain, Proceedings of the National Academy of Sciences 37 (4) (1951) 205–211. `doi:10.1073/pnas.37.4.205`.

[6] D. D. Georgiev, J. F. Glazebrook, On the quantum dynamics of Davydov solitons in protein α-helices, Physica A: Statistical Mechanics and its Applications 517 (2019) 257–269. `doi:10.1016/j.physa.2018.11.026`.

[7] A. S. Davydov, The theory of contraction of proteins under their excitation, Journal of Theoretical Biology 38 (3) (1973) 559–569. `doi:10.1016/0022-5193(73)90256-7`.

[8] A. S. Davydov, N. I. Kislukha, Solitons in one-dimensional molecular chains, Physica Status Solidi (b) 75 (2) (1976) 735–742. `doi:10.1002/pssb.2220750238`.

[9] A. S. Davydov, Solitons in molecular systems, Physica Scripta 20 (3-4) (1979) 387–394. `doi:10.1088/0031-8949/20/3-4/013`.

[10] A. S. Davydov, The role of solitons in the energy and electron transfer in one-dimensional molecular systems, Physica D 3 (1-2) (1981) 1–22. `doi:10.1016/0167-2789(81)90116-0`.

[11] A. S. Davydov, Solitons in quasi-one-dimensional molecular structures, Soviet Physics Uspekhi 25 (12) (1982) 898–918. `doi:10.1070/pu1982v025n12abeh005012`.

[12] A. S. Davydov, Quantum theory of the motion of a quasi-particle in a molecular chain with thermal vibrations taken into account, Physica Status Solidi (b) 138 (2) (1986) 559–576. `doi:10.1002/pssb.2221380221`.

[13] A. S. Davydov, Solitons in biology, in: S. E. Trullinger, V. E. Zakharov, V. L. Pokrovsky (Eds.), Solitons, Modern Problems in Condensed Matter Sciences, North-Holland, Amsterdam, 1986, pp. 1–51.

[14] A. S. Davydov, V. N. Ermakov, Linear and nonlinear resonance electron tunneling through a system of potential barriers, Physica D: Nonlinear Phenomena 28 (1) (1987) 168–180. `doi:10.1016/0167-2789(87)90127-8`.

[15] A. S. Davydov, V. N. Ermakov, Soliton generation at the boundary of a molecular chain, Physica D: Nonlinear Phenomena 32 (2) (1988) 318–323. `doi:10.1016/0167-2789(88)90059-0`.

[16] Y. S. Kivshar, B. A. Malomed, Dynamics of solitons in nearly integrable systems, Reviews of Modern Physics 61 (4) (1989) 763–915. `doi:10.1103/RevModPhys.61.763`.

[17] L. S. Brizhik, A. S. Davydov, Soliton excitations in one-dimensional molecular systems, Physica Status Solidi (b) 115 (2) (1983) 615–630. `doi:10.1002/pssb.2221150233`.

[18] L. S. Brizhik, Y. B. Gaididei, A. A. Vakhnenko, V. A. Vakhnenko, Soliton generation in semi-infinite molecular chains, Physica Status Solidi (b) 146 (2) (1988) 605–612. `doi:10.1002/pssb.2221460221`.

[19] L. S. Brizhik, Soliton generation in molecular chains, Physical Review B 48 (5) (1993) 3142–3144. `doi:10.1103/PhysRevB.48.3142`.

[20] L. S. Brizhik, A. A. Eremko, Electron autolocalized states in molecular chains, Physica D: Nonlinear Phenomena 81 (3) (1995) 295–304. `doi:10.1016/0167-2789(94)00206-6`.

[21] L. S. Brizhik, A. Eremko, B. Piette, W. Zakrzewski, Solitons in α-helical proteins, Physical Review E 70 (3) (2004) 031914. `doi:10.1103/PhysRevE.70.031914`.

[22] L. Brizhik, A. Eremko, B. Piette, W. Zakrzewski, Charge and energy transfer by solitons in low-dimensional nanosystems with helical structure, Chemical Physics 324 (1) (2006) 259–266. `doi:10.1016/j.chemphys.2006.01.033`.

[23] L. Brizhik, A. Eremko, B. Piette, W. Zakrzewski, Ratchet effect of Davydov's solitons in nonlinear low-dimensional nanosystems, International Journal of Quantum Chemistry 110 (1) (2010) 25–37. `doi:10.1002/qua.22083`.

[24] L. Cruzeiro, J. Halding, P. L. Christiansen, O. Skovgaard, A. C. Scott, Temperature effects on the Davydov soliton, Physical Review A 37 (3) (1988) 880–887. `doi:10.1103/PhysRevA.37.880`.

[25] L. Cruzeiro-Hansson, V. M. Kenkre, Localized versus delocalized ground states of the semiclassical Holstein Hamiltonian, Physics Letters A 190 (1) (1994) 59–64. `doi:10.1016/0375-9601(94)90366-2`.

[26] L. Cruzeiro-Hansson, S. Takeno, Davydov model: the quantum, mixed quantum-classical, and full classical systems, Physical Review E 56 (1) (1997) 894–906. `doi:10.1103/PhysRevE.56.894`.

[27] L. Cruzeiro, The Davydov/Scott model for energy storage and transport in proteins, Journal of Biological Physics 35 (1) (2009) 43–55. `doi:10.1007/s10867-009-9129-0`.

[28] W. C. Kerr, P. S. Lomdahl, Quantum-mechanical derivation of the equations of motion for Davydov solitons, Physical Review B 35 (7) (1987) 3629–3632. `doi:10.1103/PhysRevB.35.3629`.

[29] W. C. Kerr, P. S. Lomdahl, Quantum-mechanical derivation of the Davydov equations for multi-quanta states, in: P. L. Christiansen, A. C. Scott (Eds.), Davydov's Soliton Revisited: Self-Trapping of Vibrational Energy in Protein, Springer, New York, 1990, pp. 23–30. `doi:10.1007/978-1-4757-9948-4_2`.

[30] L. MacNeil, A. C. Scott, Launching a Davydov soliton: II. Numerical studies, Physica Scripta 29 (3) (1984) 284–287. `doi:10.1088/0031-8949/29/3/017`.

[31] A. C. Scott, Launching a Davydov soliton: I. Soliton analysis, Physica Scripta 29 (3) (1984) 279–283. `doi:10.1088/0031-8949/29/3/016`.

[32] A. C. Scott, Davydov solitons in polypeptides, Philosophical Transactions of the Royal Society of London Series A, Mathematical and Physical Sciences 315 (1533) (1985) 423–436. `doi:10.1098/rsta.1985.0049`.

[33] A. C. Scott, Davydov's soliton, Physics Reports 217 (1) (1992) 1–67. `doi:10.1016/0370-1573(92)90093-F`.

[34] B. Luo, J. Ye, Y. Zhao, Variational study of polaron dynamics with the Davydov ansätze, Physica Status Solidi (c) 8 (1) (2011) 70–73. `doi:10.1002/pssc.201000721`.

[35] J. Luo, B. Piette, A generalised Davydov-Scott model for polarons in linear peptide chains, European Physical Journal B 90 (8) (2017) 155. `doi:10.1140/epjb/e2017-80209-2`.

[36] J. Sun, B. Luo, Y. Zhao, Dynamics of a one-dimensional Holstein polaron with the Davydov ansätze, Physical Review B 82 (1) (2010) 014305. `doi:10.1103/PhysRevB.82.014305`.

[37] D. D. Georgiev, J. F. Glazebrook, Quantum tunneling of Davydov solitons through massive barriers, Chaos, Solitons and Fractals 123 (2019) 275–293. `doi:10.1016/j.chaos.2019.04.013`.

[38] L. Petzold, Automatic selection of methods for solving stiff and nonstiff systems of ordinary differential equations, SIAM Journal on Scientific and Statistical Computing 4 (1) (1983) 136–148. `doi:10.1137/0904010`.

[39] A. C. Hindmarsh, ODEPACK, a systematized collection of ODE solvers, in: R. S. Stepleman, M. Carver, R. Peskin, W. F. Ames, R. Vichnevetsky (Eds.), Scientific Computing, IMACS Transactions on Scientific Computation, North-Holland, Amsterdam, 1983, pp. 55–64.

[40] A. C. Hindmarsh, L. R. Petzold, Algorithms and software for ordinary differential equations and differential-algebraic equations, Part II: Higher-order methods and software packages, Computers in Physics 9 (2) (1995) 148–155. `doi:10.1063/1.168540`.

[41] M. Trott, The Mathematica GuideBook for Numerics, Springer, New York, 2006. `doi:10.1007/0-387-28814-7`.

[42] L. S. Brizhik, Influence of electromagnetic field on soliton-mediated charge transport in biological systems, Electromagnetic Biology and Medicine 34 (2) (2015) 123–132. `doi:10.3109/15368378.2015.1036071`.

[43] K. Itoh, T. Shimanouchi, Vibrational spectra of crystalline formamide, Journal of Molecular Spectroscopy 42 (1) (1972) 86–99. `doi:10.1016/0022-2852(72)90146-4`.

[44] N. A. Nevskaya, Y. N. Chirgadze, Infrared spectra and resonance interactions of amide-I and II vibrations of α-helix, Biopolymers 15 (4) (1976) 637–648. `doi:10.1002/bip.1976.360150404`.

[45] Y. Lai, H. A. Haus, Quantum theory of solitons in optical fibers. I. Time-dependent Hartree approximation, Physical Review A 40 (2) (1989) 844–853. `doi:10.1103/PhysRevA.40.844`.

[46] Y. Lai, H. A. Haus, Quantum theory of solitons in optical fibers. II. Exact solution, Physical Review A 40 (2) (1989) 854–866. `doi:10.1103/PhysRevA.40.854`.

[47] E. M. Wright, Quantum theory of self-phase modulation, Journal of the Optical Society of America B 7 (6) (1990) 1142–1146. `doi:10.1364/josab.7.001142`.

[48] R. J. Glauber, The quantum theory of optical coherence, Physical Review 130 (6) (1963) 2529–2539. `doi:10.1103/PhysRev.130.2529`.

[49] R. J. Glauber, Coherent and incoherent states of the radiation field, Physical Review 131 (6) (1963) 2766–2788. `doi:10.1103/PhysRev.131.2766`.

[50] D. D. Georgiev, J. F. Glazebrook, Neurotransmitter release and conformational changes within the SNARE protein complex, in: S. E. Lyshevski (Ed.), Nanoengineering, Quantum Science, and, Nanotechnology Handbook, CRC Press, Boca Raton, 2019, pp. 375–404.

[51] L. S. Brizhik, J. Luo, B. M. A. G. Piette, W. J. Zakrzewski, Long-range donor-acceptor electron transport mediated by α-helices, Physical Review E 100 (6) (2019) 062205. `doi:10.1103/PhysRevE.100.062205`.

[52] T. Takei, K. Tsumoto, A. Okonogi, A. Kimura, S. Kojima, K. Yazaki, T. Takei, T. Ueda, K. Miura, pH responsiveness of fibrous assemblies of repeat-sequence amphipathic α-helix polypeptides, Protein Science 24 (5) (2015) 883–894. `doi:10.1002/pro.2665`.

[53] D. P. Ng, C. M. Deber, Modulating transmembrane α-helix interactions through pH-sensitive boundary residues, Biochemistry 55 (31) (2016) 4306–4315. `doi:10.1021/acs.biochem.6b00380`.

[54] Z. Fezoua-Boubegtiten, B. Hastoy, P. Scotti, A. Milochau, K. Bathany, B. Desbat, S. Castano, R. Oda, J. Lang, The transmembrane domain of the SNARE protein VAMP2 is highly sensitive to its lipid environment, Biochimica et Biophysica Acta (BBA) - Biomembranes 1861 (3) (2019) 670–676. `doi:10.1016/j.bbamem.2018.12.011`.

[55] R. P. Feynman, Space-time approach to non-relativistic quantum mechanics, Reviews of Modern Physics 20 (2) (1948) 367–387. `doi:10.1103/RevModPhys.20.367`.

[56] R. P. Feynman, A. R. Hibbs, Quantum Mechanics and Path Integrals, McGraw-Hill, New York, 1965.

[57] T. Kashiwa, Y. Ohnuki, M. Suzuki, Path Integral Methods, Oxford University Press, Oxford, 1997.

[58] D. D. Georgiev, E. Cohen, Probing finite coarse-grained virtual Feynman histories with sequential weak values, Physical Review A 97 (5) (2018) 052102. `doi:10.1103/PhysRevA.97.052102`.

[59] S. K. Kolev, P. S. Petkov, M. Rangelov, G. N. Vayssilov, Ab initio molecular dynamics of Na^+ and Mg^{2+} countercations at the backbone of RNA in water solution, ACS Chemical Biology 8 (7) (2013) 1576–1589. `doi:10.1021/cb300463h`.

[60] S. K. Kolev, P. S. Petkov, M. A. Rangelov, D. V. Trifonov, T. I. Milenov, G. N. Vayssilov, Interaction of Na^+, K^+, Mg^{2+} and Ca^{2+} counter cations with RNA, Metallomics 10 (5) (2018) 659–678. `doi:10.1039/c8mt00043c`.

[61] D. Hennig, Energy transport in α-helical protein models: one-strand versus three-strand systems, Physical Review B 65 (17) (2002) 174302. `doi:10.1103/PhysRevB.65.174302`.

[62] E. Lindahl, Molecular dynamics simulations, in: A. Kukol (Ed.), Molecular Modeling of Proteins, Vol. 1215 of Methods in Molecular Biology, Springer, New York, 2015, pp. 3–26. `doi:10.1007/978-1-4939-1465-4_1`.

[63] P. E. M. Lopes, O. Guvench, A. D. MacKerell, Current status of protein force fields for molecular dynamics simulations, in: A. Kukol (Ed.), Molecular Modeling of Proteins, Vol. 1215 of Methods in Molecular Biology, Springer, New York,

2015, pp. 47–71. doi:10.1007/978-1-4939-1465-4_3.

[64] M. Khalili, A. Liwo, F. Rakowski, P. Grochowski, H. A. Scheraga, Molecular dynamics with the united-residue model of polypeptide chains. I. Lagrange equations of motion and tests of numerical stability in the microcanonical mode, Journal of Physical Chemistry B 109 (28) (2005) 13785–13797. doi:10.1021/jp058008o.

[65] M. Khalili, A. Liwo, A. Jagielska, H. A. Scheraga, Molecular dynamics with the united-residue model of polypeptide chains. II. Langevin and Berendsen-bath dynamics and tests on model α-helical systems, Journal of Physical Chemistry B 109 (28) (2005) 13798–13810. doi:10.1021/jp058007w.

[66] M. Chernodub, S. Hu, A. J. Niemi, Topological solitons and folded proteins, Physical Review E 82 (1) (2010) 011916. doi:10.1103/PhysRevE.82.011916.

[67] N. Molkenthin, S. Hu, A. J. Niemi, Discrete nonlinear Schrödinger equation and polygonal solitons with applications to collapsed proteins, Physical Review Letters 106 (7) (2011) 078102. doi:10.1103/PhysRevLett.106.078102.

[68] A. Krokhotin, A. J. Niemi, X. Peng, Soliton concepts and protein structure, Physical Review E 85 (3) (2012) 031906. doi:10.1103/PhysRevE.85.031906.

[69] A. Krokhotin, M. Lundgren, A. J. Niemi, Solitons and collapse in the λ-repressor protein, Physical Review E 86 (2) (2012) 021923. doi:10.1103/PhysRevE.86.021923.

[70] A. Krokhotin, A. Liwo, G. G. Maisuradze, A. J. Niemi, H. A. Scheraga, Kinks, loops, and protein folding, with protein A as an example, Journal of Chemical Physics 140 (2) (2014) 025101. doi:10.1063/1.4855735.

[71] N. Taghizadeh, M. Mirzazadeh, F. Farahrooz, Exact solutions of the nonlinear Schrödinger equation by the first integral method, Journal of Mathematical Analysis and Applications 374 (2) (2011) 549–553. doi:10.1016/j.jmaa.2010.08.050.

[72] N. Taghizadeh, Q. Zhou, M. Ekici, M. Mirzazadeh, Soliton solutions for Davydov solitons in α-helix proteins, Superlattices and Microstructures 102 (2017) 323–341. doi:10.1016/j.spmi.2016.12.057.